DYNAMIC STATISTICS OF CRAYFISH CAUDAL PHOTORECEPTORS

HOWARD T. HERMANN *and* RICHARD E. OLSEN

From the Neurophysiology Laboratory, McLean-Massachusetts General Hospital, Belmont, Massachusetts

ABSTRACT Crayfish caudal photoreceptor units were monitored during transient and steady-state responses to light stimuli (step on, step off). A statistical analysis of interpulse interval distributions during quasi-stationary time periods was carried out. Firing statistics during transient conditions were superposable with statistics under whatever steady stimulation produced the same firing rate, indicating that mean firing rate is a sufficient statistic. Distributions encountered formed a continuum of possible shapes. Considerable variation in shape was found with temperature and also among species, with *Orconectes clarkii* tending to fire more regularly than *Orconectes virilis*. Some properties of *O. virilis* statistics are described, including a linear relation between mean and standard deviation, and a tendency for intervals to be nonindependent.The data are considered as constraints on closed form models of the photoreceptor nerve pulse generator.

INTRODUCTION

This is the first in a series of papers attempting to characterize a neural message. Such characterization requires that the neural events comprising the message be amenable to exhaustive monitoring. Further, the message should be part of a system with a well-defined behavioral response. Within the system itself, it is also desirable that the decision element, which detects the arrival of the message, be accessible to probing (1).

The negative phototropic walk response exhibited by the crayfish qualifies well as an experimental paradigm. When other sensory modalities are controlled, and with control over ambient light, walking activity can be triggered by photic stimulation of the sixth caudal ganglion (2, 3). This tropism may be described as a stochastic decision process. The neural information resultant from such stimulation can be exhaustively monitored (4); the walk response is unambiguous; and the esophageal brain, containing the decision element, is readily accessible to probing.

Anatomy and Physiology

Embedded, one on each side, in the milky neuropil of the abdominal (caudal) ganglion of the crayfish, lie the two photosensitive neural units whose message we

wish to study (5, 6). Their sensitivity curve peaks at 500 mμ, resembling curves for human rhodopsin (7, 8). In both afferented and deafferented preparations, their light-to-nerve pulse transfer function may be approximated by a linear, second order, critically damped lag element whose break frequency lies around 0.12 Hz. This transfer function holds true only for small signal perturbation, large forcing functions producing overshoot. The message passes cephalad to the esophageal brain without synapse (9).

The message to the brain appears to be conveyed in the transient; steady levels of light show no effect on walking behavior (3). Accordingly, statistical analysis of signal content of transient, as well as steady state, were believed to be valuable in assessing the centrally directed message. The present paper is restricted to the statistical characterization of the intact, in situ preparation.

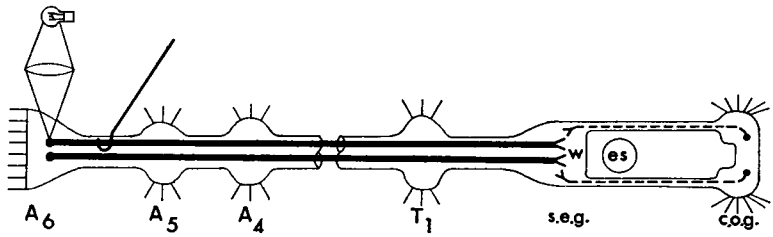

FIGURE 1 Schematic representation of crayfish nervous system, indicating site of stimulation and recording. Paired photounits are located in caudal (sixth abdominal) ganglion, and communicate without synapse to the subesophageal ganglion (s.e.g.). Hook represents position of recording electrodes. Walking is controlled in the subesophageal ganglion, but is affected by signals (dotted lines) from the cerebral optic ganglion (c.o.g.) as well as by the caudal photoreceptor. (es) is esophageal hiatus through ganglion. There are three abdominal and four thoracic ganglia (not depicted) between A_4 and T_1.

METHOD

The ventral nerve cord of the abdomen, exposed by removal of the overlying translucent exoskeleton, was severed between A_1 and A_2, care being taken to preserve the ventral artery. After the A_6 ganglion was shielded from light, the tough protective sheath encasing the cord was slit from A_5 to A_6 with the point of a razor shard. A slender nerve fascicle containing the photounit fiber was then dissected free with a sharpened glass needle (4). The choice of fascicle was monitored for light-fiber content on a CRT. This fascicle was then serially split until it met the criteria for single-unit recording (see Data Processing Sequence, below). At this point, the fiber generally appeared as a homogeneous filament under the viewing microscope; occasionally a filament pair was used. All roots to the ganglion were left untouched. See Fig. 1 for experimental arrangement.

Bipolar electrodes of 50 μ platinum-irridium wire led to a conventional high-gain ac amplifier whose pass band extended from 35 Hz to 2k Hz. The dissecting and recording area was a fully grounded cage fashioned from 0.125 inch magnetic stainless steel. It provided an effective shield against stray ambient light and electrical fields as well as a universal mounting place for magnetic chucks (by which all mechanical systems were fastened to the cage). During experiments, the cage was maintained typically at a temperature of 17°C (65°F) and

the atmosphere saturated with water vapor. Under these conditions, a preparation would be stable for more than 20 hr.

Photic stimulation was restricted to step changes in light intensity. Light from a tungsten lamp (driven by a regulated, constant-current source) was collimated and passed through an interference filter centered on 502.2 mμ, with half-power points at 501.5 and 503.0 mμ. Spectral content was relatively invariant to tungsten temperature in the range employed. Flux was monitored from the collimated beam by a phototube system calibrated from a standard light source, and was maintained at fractions of 12.6 mlm/cm² on the ganglion. Levels were reduced stepwise to ~0.09 mlm/cm² by means of neutral density filters.

Experimental sequences were arranged to counter any long-term effects of stimulation or fatigue. Light presentations were separated by dark recovery periods of at least 20 min, which reestablished initial conditions. Stimuli were light pulses (step on, step off) of 2–5 min duration.

Since the receptor's response is never quite the same each time the stimulus is applied, the same stimulus condition was repeated a number of times over the course of the experiment, and an average pulse interval histogram obtained. In general, low intensities showed more variability and, accordingly, were repeated two or three times as frequently as the high intensity stimuli. Responses were monitored for signs of deterioration, and if similar stimuli did not show similar statistics in shuffled sequences, the preparation was discarded. In all, 35 preparations met criterion.

Data Processing Sequence

Amplified nerve pulses were passed through a pulse amplitude-sensitive "window" of our own design,[1] which generated a short marker pulse for every nerve pulse that fell within the window; it excluded all pulses above or below the window settings. The settings were monitored on a storage CRT. Occasional errors due to superposition of the desired pulse with unwanted pulses occurred, but preparations were accepted only if the estimated error was <1%. Noise was ~6 μv pp, and the signals ranged from 200 μv to 2 mv pp, so errors due to superposition of noise were virtually nonexistent. (The window size was not less that 20% of the pulse amplitude.) Both raw data and shaped pulses, as well as the light monitor, were stored on FM tape. Shaped pulses were processed by a special purpose digital computer of our own design and construction, utilizing a clock pulse, digital counter, gates, and registers. The computer generated interval histograms and pairwise dependency plots. In addition, on-line displays[1] of "instantaneous" mean and variance were monitored on a storage CRT face. Our experiments lasted from 12 to 24 hr, during which stationarity could be conveniently monitored both by the computer-generated histograms and an instantaneous interval plot device.[1]

RESULTS

1. Anatomy

In keeping with the reported anatomic locus in the ventral cord (10, 6) constancy of position was encountered. In *Orconectes virilis*, the left unit was always immediately lateral to the midline and at the ventral surface in Wiersma's area 82. The right unit was probably equally constant, but being more centrally located (Wiersma area 79 or 80), it was more difficult to pinpoint.

[1] To be reported elsewhere.

2. *Steady-State Afferented Firing Patterns*

In darkness, afferented photoreceptor firing shows a characteristic pattern of pairs or groups of pulses, separated by relatively long intervals (insert, Fig. 2 a). Most units produce pulse pairs, although triplets and even quadruplets have been observed. The interval between the first and second pulses is close to the absolute refractory period (5–7 msec); no shorter intervals are seen under any conditions. Most coupled pulses fall in the relative refractory period, as indicated by a reduced height of the

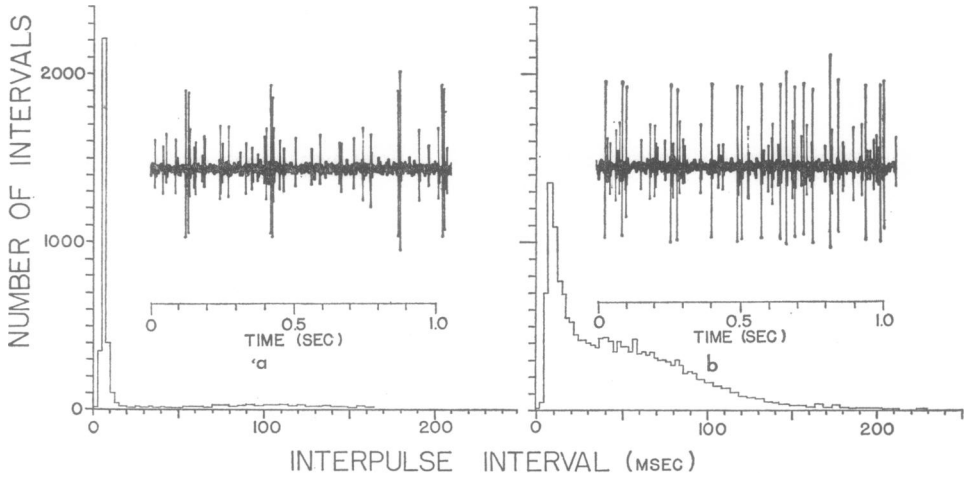

FIGURE 2 Sample CRT tracings and respective pulse interval histograms of a typical *Orconectes virilis* caudal (A_6 ganglion) photoreceptor unit, recording from nerve filament between A_5 and A_6. The largest nerve pulses are from the photoreceptor; the smaller are typically from mechanoreceptors. Preparation 1445; histogram averaging epoch, 16 min. (a) dark-adapted state. Pulse pairs, typical of resting pattern, dominate record. In records not corrupted by other pulses, the second of the pair is always smaller. Pairing interval (5–7.5 msec) and pair repetition interval (~120 msec) may be seen respectively in the sharp and broad peaks of the corresponding PIH. (b) photic driving, 0.5 mlm/cm² steady illumination. Light-driven response overrides pairing giving fairly random firing pattern. Continued presence of sharp, short and broad, long peaks in the histogram indicate (but do not prove) that some pairing persists.

second pulse. When triplets and quadruplets occur, the additional pulses follow at intervals slightly longer than that of the initial pair. A pulse interval histogram of dark resting activity reflects these patterns. The *n*-tuplets peak the distribution in the short interval range (5–10 msec) (Fig. 2 a). The broad peak in the 120 msec range reflects the intervals between *n*-tuplets.

Light stimulation contracts the mean interval and simultaneously reduces the number of both very short and very long intervals. The nerve pulse sequence now resembles a random process (insert, Fig. 2 b). The pulse interval histogram reflects this change (Fig. 2 b).

There is some variation among animals in the shape of the light-driven steady-state pulse interval histogram. Fig. 3 a-c illustrates the range encountered. A con-

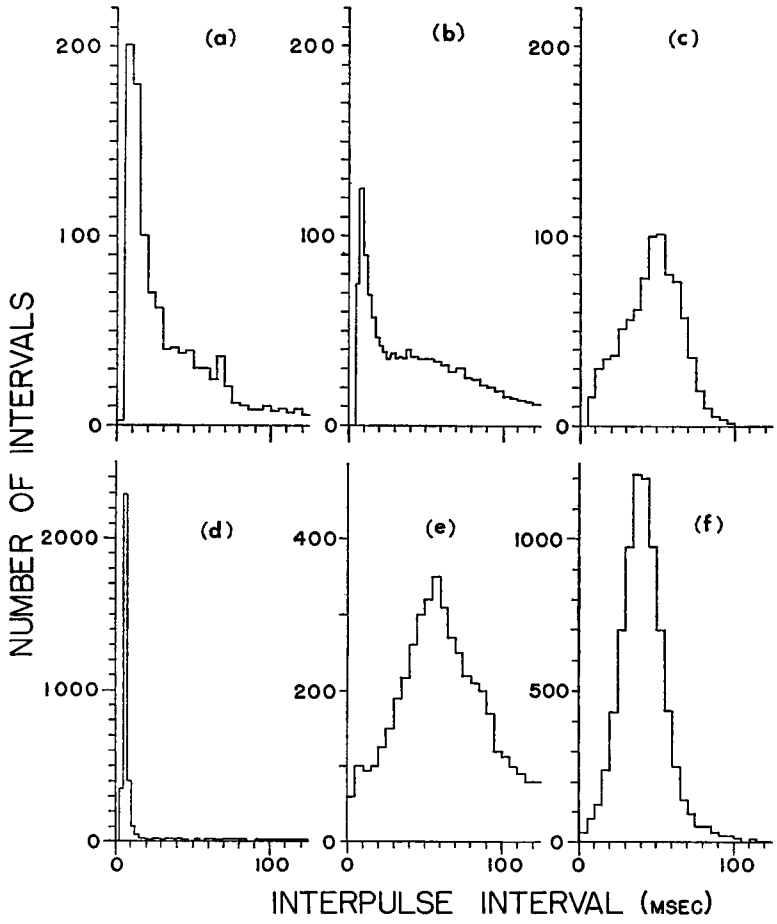

FIGURE 3 Sample histograms showing varieties of steady-state distributions encountered. Vertical dimensions are scaled arbitrarily to aid visual comparison. Units a-c are 3.0 mlm/cm² steady illumination; histogram epoch is 40 sec. (a) type A, "Quasi-Poisson." (b) type B, "Mixed." Compared with type A has a broad hump in 40–60 msec range. This type characterized the majority of *O. virilis* preparations. (c) type C, "Quasi-Gaussian." Encountered rarely in *O. virilis*. (d) dark resting state, 16 min epoch length, *O. virilis*. Units e–f are *O. clarkii*, epoch length of 5.3 min. (e) dark resting state; quasi-Gaussian distribution and high resting rate are typical. (f) 3.0 mlm/cm² steady illumination. *O. clarkii* show less modulation sensitivity than *O. virilis*.

tinuum of possibilities exists between those shown; however, most units encountered were distributed between types A (Fig. 3 a) and B (Fig. 3 b). Preparations in some-way damaged tended to produce statistics like C (Fig. 3 c), but some seemingly intact and quite stable units also did. For comparison, a dark resting PIH (Pulse Interval Histogram) is shown in Fig. 3 d. In particular, *Orconectes clarkii*[2] never

[2] Obtained from the Louisiana Game and Fisheries Department.

showed the quasi-Poisson distributions of type A, nor even the type B distribution. They all tended to a quasi-Gaussian type C PIH. Further, the dark resting rate was much higher and the distribution less dominated by pairings (Fig. 3 e, f).

Since temperature dependence of distributions in isolated crayfish caudal neurons has been described (11), a short study was made of the intact unit to determine the importance of temperature in the shape variation observed. The results are still preliminary, but one unit, A type at 59°F, produced "C" type distributions at 70°F. That most experiments were run at about 60–65°F may explain the preponderance of A and B units found.

In some cases, recording was done from both the right and left photounits simultaneously. The interval distributions were found to be similar but not identical between the two units. For example, in Fig. 4 the left unit is consistently slightly faster than the right, but the PIH shapes are not significantly different.

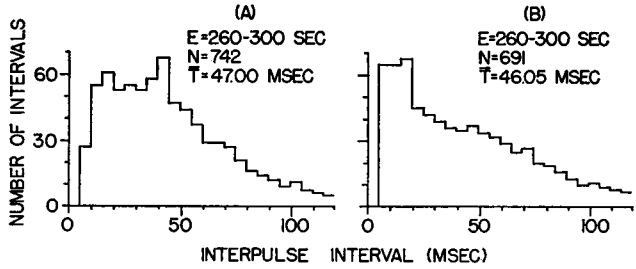

FIGURE 4 Comparison of right- and left-sided units in same animal stimulated at 3.0 mlm/cm², and simultaneously recorded over a 40 sec steady-state period. (E = histogram epoch; N = events in histogram; $\bar{T}$ = mean of histogram.) (A) PIH of left unit tends to a type C distribution. Its N (number of pulses represented) of 742 shows its greater sensitivity to light. (B) right side unit type B distribution with N of 691. *O. virilis*, 11245.

3. Transient Responses

In response to a step change of light from dark levels, the nerve exhibits a latent period of 1 or 2 sec followed by a rapid rise of the mean rate (fall in the mean interval), which overshoots and gradually returns to the new steady-state level. The responses to step increases and step decreases are similar, although response to a step decrease occurs more gradually and has a protracted undershoot.

Study of the firing pattern of the photounit during transients has been of central interest to us. Two problems appeared attendant to the choice of an appropriate study vehicle: (*a*) "pattern" is not a measurable quantity. Nonetheless, during illumination, one interspike interval depends very little on preceding intervals, so that pattern could be said to exist as the distribution function of intervals (Pulse Interval Histogram). (*b*) change in pattern is even more difficult to describe in any quantitative sense. Since most statistical characterizations assume stationarity of the random process under scrutiny and stationarity implies an infinite sample

length, a quasi-stationarity must be established. If selected samples of the nerve pulse train are brief (differentially constant) with respect to the time course of the transient but sufficiently long with respect to the number of intervals represented in the time slice to be a good estimator of the process, quasi-stationarity may be assumed during the sample length. The result is a series of pulse interval histograms, each representing a successive slice (epoch) in time. In some cases a stimulation condition was repeated several times. A shorter epoch could then be used and the individual results summed. Histograms were normalized to the same epoch length (5 sec.).

A photoreceptor transient response analyzed in this way is shown in parts B through L of Fig. 5. Stimulation is the sudden onset of light at 12.6 mlm/cm^2. At the end of the latent period ($\sim$2 sec), the unit crescendos into an intense, almost regular firing, with no long intervals and relatively few very short ones. There follows a period during which long intervals remain infrequent, and both short and medium intervals are equally likely. Finally, in the steady state, the diminution of moderate intervals and reappearance of long ones establishes an almost exponential distribution. Steady state is achieved approximately 60 sec after the onset of light. (For later analytical purposes we conservatively define steady state as the period beyond 3 min.) Beyond this point no shape change occurred, although the mean firing rate decays slightly over hours, particularly with continued intense stimulation. Fig. 6 is typical.

4. Intensity Dependence

The PIH changes shape not only as a function of time, but also as a function of intensity of stimulus. Fig. 7 illustrates a typical case of this for a class B unit. At low intensities in the steady state one sees a short, sharp refractory period, a narrow peak followed by a broad hump and a slow exponential final tail. At higher intensities, relative refractoriness extends farther out, limiting the shorter intervals and causing an outward shift in the mode (most probable interval). More pulses also appear in the short intervals, resulting in a broader peak and less noticeable humping. Consistent with the higher mean, there is a faster exponential tail at greater intensities. As a result, the higher the intensity, the more the unit approaches the oft used Poisson-with-refractory period distribution. At lower illumination, the fit to this model becomes quite poor.

We have studied the transient response at various intensities in order to complete the characterization of the photounit light response. Although histograms differ among animals, the transformations which the distributions undergo in such experiments show general consistencies.

Initially (5–10 sec), all distributions appear exponential, with high peaks at short intervals, and few moderately long intervals. The mode is located at longer intervals as illumination is increased, except for the most intense stimuli, where it is driven shorter again (Fig. 8). At 15–20 sec after onset of stimulus, shapes have changed

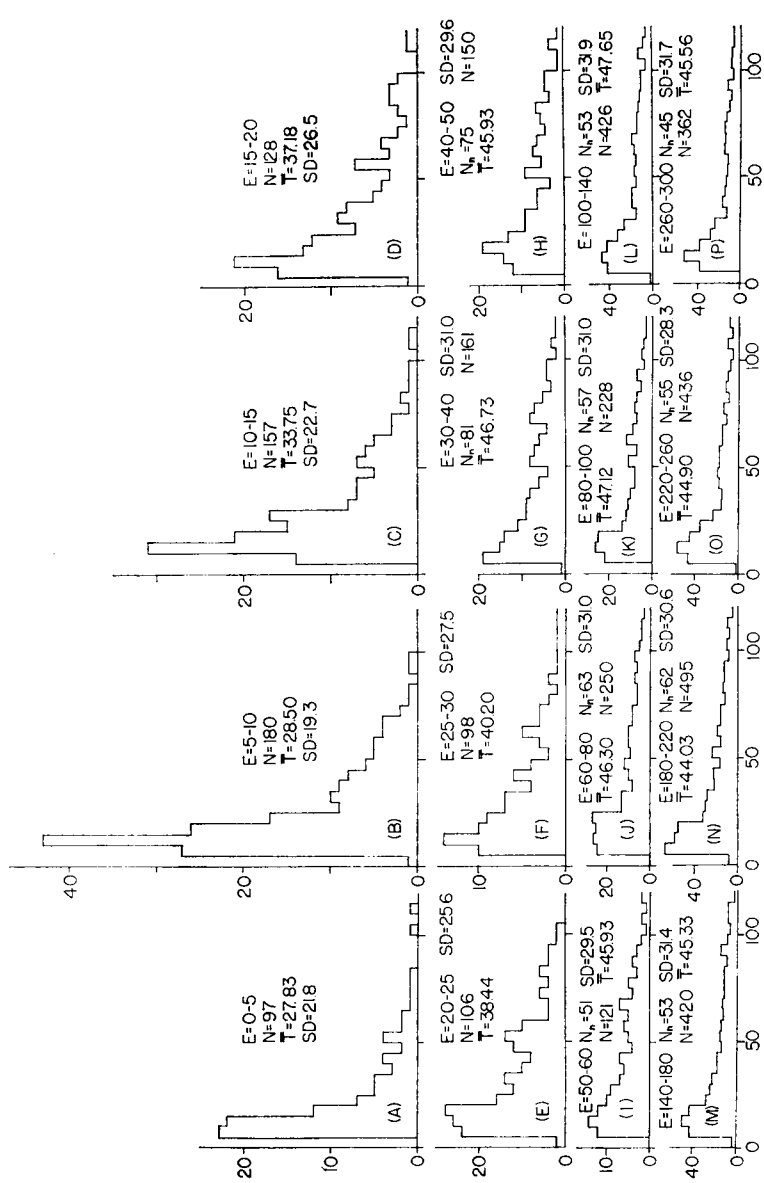

FIGURE 5 Response (in terms of interpulse interval statistics) of photounit to step-change of illumination from 30-min dark-adapted state to 2.9 ml/cm². *O. virilis* 11125. (A–L) pulse interval histograms prepared from successive epochs of time following onset of stimulus. *E*, epoch during which statistics are represented, in seconds from light onset; *N*, number of pulses represented in PIH; N_n, *N* normalized to adjust for lengthening of epochs; $\bar{T}$, mean, SD, and standard deviation of histogram. Both mean and standard deviation increase with time; the mode shifts out slightly during transient but is erratic. Relaxation to steady state appears to be complete by 60 sec.

considerably. The distributions for all intensities have exponential tails, although at lower intensities secondary "humping" occurs. In addition, at low intensities (0.9 mlm/cm²), the location of the mode is inconsistent. As time continues (40–50 sec), the location of the humps continues to shift out for all intensities, giving rise to flat sections at lower intensities, and broader peaks at higher ones. In any one epoch, the hump appears at shorter intervals for more intense stimuli. The rate at which the distributions relax to steady state seems not to be a function of intensity.

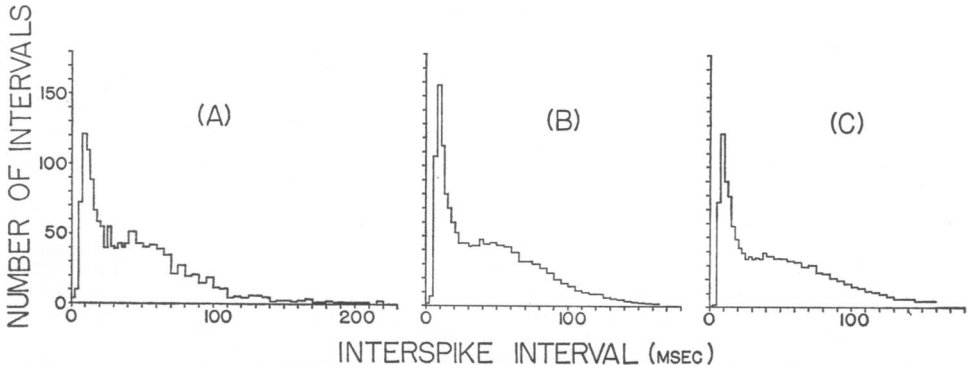

FIGURE 6 Stationarity of pulse interval histograms after relaxation of transient. (A) 1-min averaging epoch starting at 5th minute. (B) 16 min epoch starting at 20th min. (C) 16 min epoch starting at 50th min. Histograms are normalized to match 5–6 min epoch. Illumination: 0.5 mlm/cm². *O. virilis*, 04145. Stationarity is good as indicated by similarity in shape of PIH and comparability of mean rate.

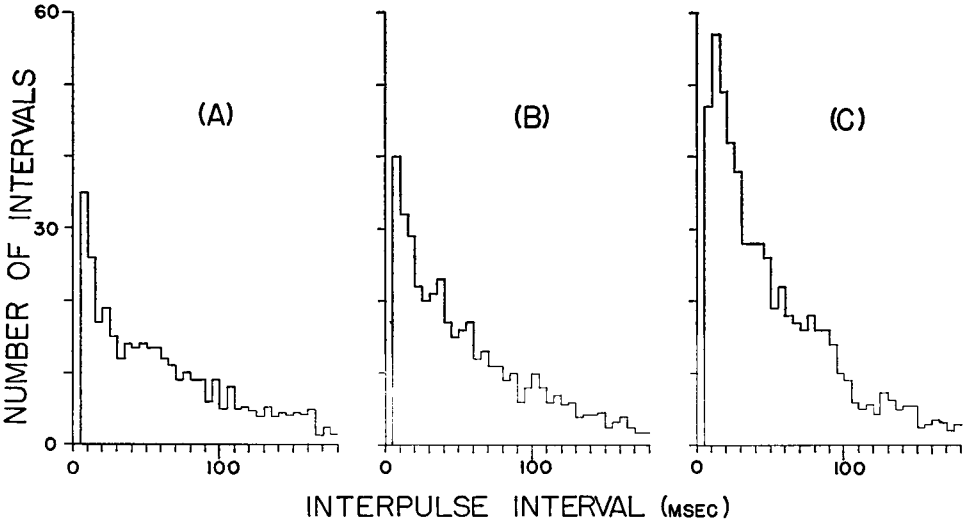

FIGURE 7 Variation in histogram shape as a function of intensity. Steady illumination, 40 sec epoch, 5-min after onset of light. Illumination levels are (A) 0.9, (B) 3.0, (C) 12.6 mlm/cm². Unit is classified as B type owing to appearance of hump in moderate interval range at low intensity of stimulation. *O. virilis*, 10305.

5. *Histogram Shape Invariance*

An interesting comparison may be made if we apply a photic step increase, not from dark, but from some lower steady-state level. An experiment of this type is illustrated in Fig. 9. The animal is experiencing a smaller change (0.90–12.6 mlm/cm²) and the transient is correspondingly less pronounced. It appears, in fact, quite similar to another stimulation given the same unit (Fig. 5), one from dark to one-

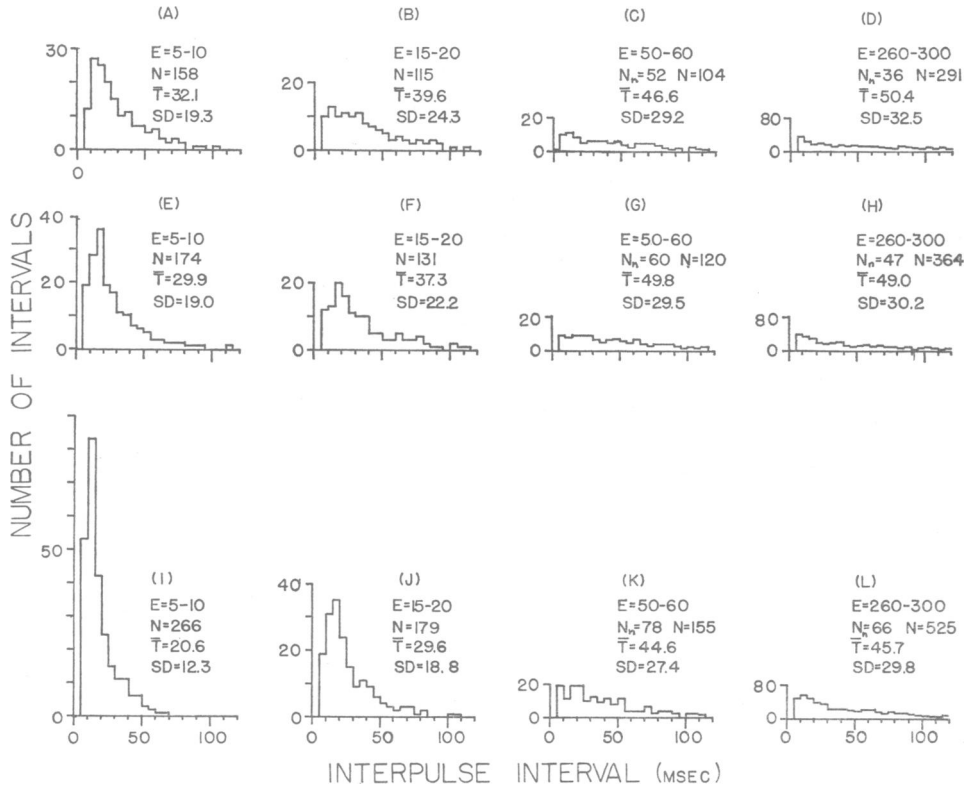

FIGURE 8 Transient pulse statistics at three illumination levels. Each row represents the time course of response of unit at one level of stimulation. Time sequences of transients read serially from left to right. Stimuli were: A–D, 0.9 mlm/cm²; E–H, 3.0 mlm/cm²; I–L, 12.6 mlm/cm², steady illumination following dark adaptation. For symbols, see Fig. 4. *O. virilis*, unit 10305.

fourth the intensity (0.0–2.95 mlm/cm²) of that shown in Fig. 9. The light-adapted case of Fig. 9 relaxes toward steady state no faster than the dark-adapted response.

A stronger and more surprising invariance may be noted by comparing all histograms which manifest the same mean, but come from experiments having different stimulus conditions. For example, identical means may be found in steady-state high intensity and during peak transient response at low intensity, or steady-state

moderate intensity and late transient lower intensity, and so on. Regardless of the stimulus conditions, histograms with similar means show similar shapes. An example of this may be seen in Fig. 10. Here, the PIH at 15–20 sec for high intensity has the same mean as the 5–10 sec PIH at moderate intensity, and the shapes are the same. This feature, that PIH having the same mean have the same shape, appears in all of our data as characteristic of the photounits.

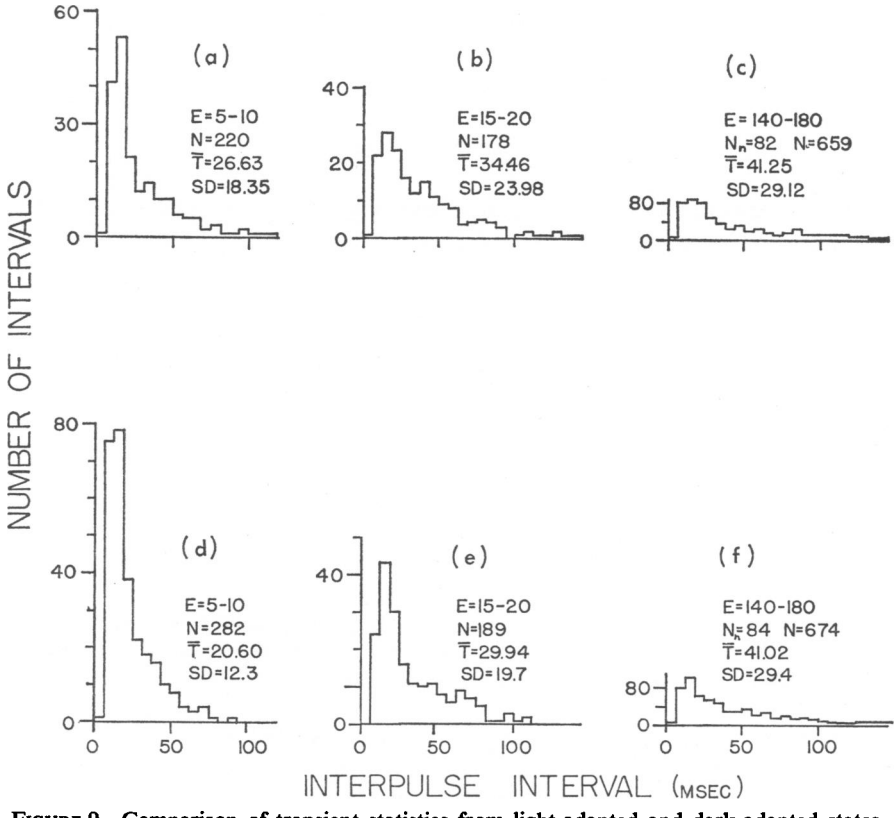

FIGURE 9 Comparison of transient statistics from light-adapted and dark-adapted states. In both cases, stimulation is a step increase of light to 12.6 mlm/cm². Conditioning is (a) 10 min of 0.9 mlm/cm²; (b) 30 min of darkness. *O. virilis*, unit 11125.

Such a statement is necessarily subjective since it involves statistical variation and the naked eye comparison of shapes. As a further test, we have plotted the standard deviation of intervals against the mean (Fig. 11). One can see that regardless of change in amplitude of forcing function, or of transient as opposed to steady state, the standard deviation bears a fixed relationship to the mean, namely $\log \bar{T} = M \log \sigma$. It should be emphasized that to support the hypothesis that shape is only a function of mean, it is necessary but not sufficient that for each mean there be a unique standard deviation.

DISCUSSION

Given a mass of pertinent data, we would prefer to reduce it to some closed-form model. The particular system which we wish to model here is the photoreceptor input-output transfer function, although not necessarily a transfer function in the linear system theory sense. One simple form of modeling is to consider the output to be completely characterized in terms of one parameter, for example, the mean rate, which is then related to the stimulus by an appropriate equation. Hermann and Stark (4) gave a fit to caudal photoreceptor response in terms of linear system theory, with the Laplace transform

$$G(s) = G(0)\,\frac{e^{-1.0\,s}}{(1 + 1.3s)^2}.$$

They noted, however, that for sinusoidal intensity input, the mean output did not vary sinusoidally when the variation was large. Kennedy (6) and Uttal and Kasprzak

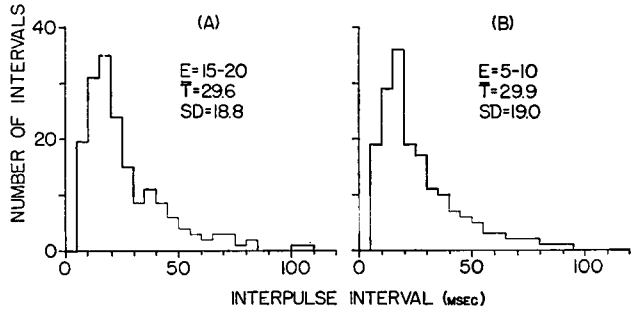

FIGURE 10 Statistics with equal means, but under different stimuli. PIH's selected from Fig. 8. (A) sample epoch 15–20 sec at 12.6 mlm/cm². (B) sample epoch 5–10 sec at 3.0 mlm/cm². *O. virilis*, unit 10305. PIH's with similar means have similar distributions.

(7) noted typical sensory receptor nonlinearities in the plots of intensity of input vs. nerve pulse output rate. All these are inconsistent with linear analysis. One way of removing the defect is to postulate a nonlinear but memoryless mechanism attached to the output of a linear system. In effect, this defines a new scale for the output, in terms of which the input-output relation is linear. The modification, however, still does not give an adequate model, for Hermann and Stark found phase shift to vary with amplitude, and our data shows the "off" response to take place at a slower rate than the "on" response, both of which imply nonlinearity in time relationships. A possible final alternative along these lines is to use a nonlinear differential equation, a difficult problem, and well beyond the scope of this work.

Another approach, which we consider to be more rewarding, is the following. We shall consider the generated nerve signal to be a sample function of an ergodic random process whose statistical parameters vary with the fluctuations of photic energy striking the receptor. A stochastic process is strictly specified by the cumula-

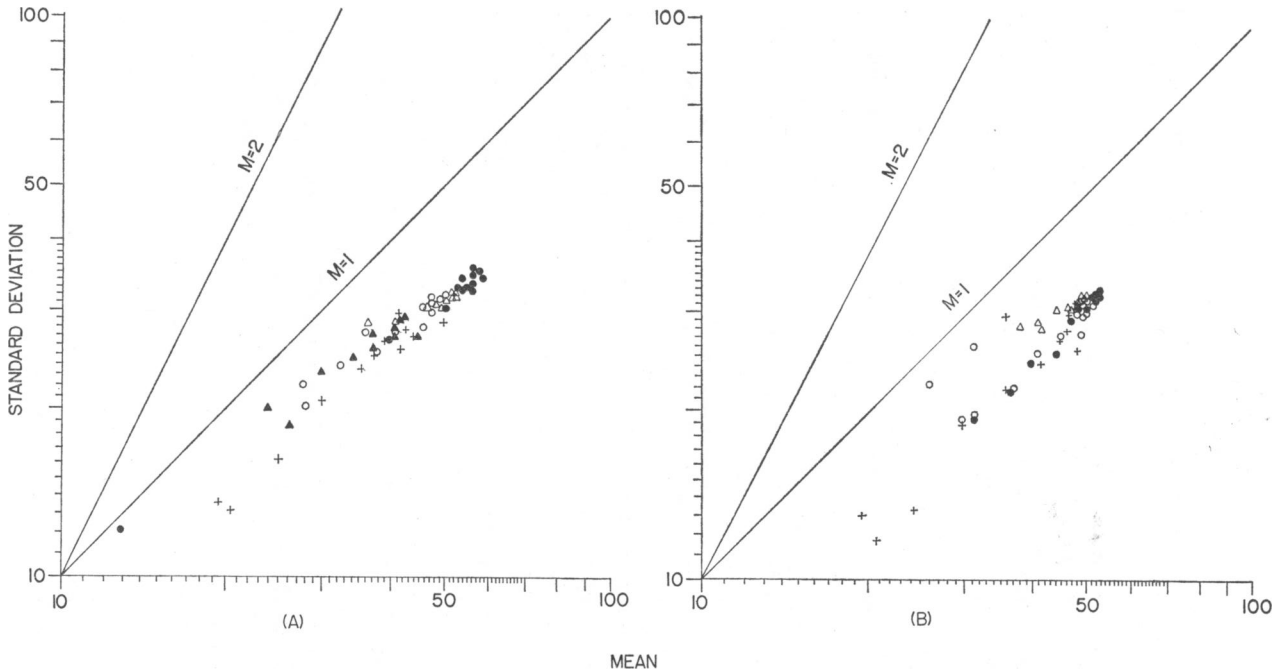

FIGURE 11 Log-log plots of interval standard deviation vs. interval mean. Each graph represents one photounit. Data are from four light levels (dark, 0.9, 3.0, and 12.6 mlm/cm^2), under both transient and steady-state conditions. Sample epochs for transients are in format of Fig. 5. A straight line of slope $M = 1$ gives the relation $\sigma = kt$, with (A) Unit 11125, $k = 0.75$; (B) Unit 10305, $k = 0.68$.

tive probability distribution functions $[P_j(t)]$, where if the jth event occurs at time t_j,

$$P_j(t) \triangleq P[t_j \leq t | t_{j-1}, \cdots, t_0].$$

If we assume stationarity, it is adequate to specify the $[P_j(s)]$ (where s = time since last pulse), since if $\tau_j = t_j - t_{j-1}$,

$$P_j(t) = P[t_j \leq t | t_{j-1}, \cdots, t_0] = P[\tau_j \leq s_j | \tau_{j-1}, \cdots, \tau_0] = P_j(s).$$

Another assumption, much less justifiable a priori, but often made in studies of this type, is independence of all intervals, or

$$P_j(t) = P[t_j \leq t | t_{j-1}, \cdots, t_0] = P[\tau \leq s] = P(s).$$

If, therefore, the two assumptions are valid, the distribution of τ's or intervals in a signal generated by a neuron is a good estimator of the appropriate stochastic process. In terms of experimental observations, the τ or pulse interval histogram (PIH) would converge (in the limit of an infinitely long sample) to $f(s)$, where

$$f(s) = \frac{dP(s)}{ds}.$$

As an alternative to specifying the probability functions, we may specify a stochastic-generating algorithm, some parameters of which are functions (hopefully linear) of the stimulus. Along such lines, certain features of our data are seen to impose constraints on candidate models:

1. The mode varies as a function of intensity and time. It tends to be least when the mean is lowest and highest.

2. For long intervals, the distribution falls off exponentially. In cases such as the transients, experimental sample populations are too small for this to be defined with certainty.

3. Under some conditions the distribution has a secondary maximum at moderate intervals, in addition to the one at short intervals. This may be a true maximum, but more often is a flat section, or an area far from the initial peak which does not fit the exponential, long interval tail.

4. Adjacent intervals are not independent in distributions having secondary humps. This is quite evident in the paired firing of the unit in the dark (Fig. 2 a, insert), whose typical PIH distribution was shown in Fig. 2 a. A light response shown in Fig. 3 b shows similar features. Its joint interval histogram (JIH) in Fig. 12 indicates that this is due to interinterval dependencies.

A possible insight into the process which generates these "humps" may be gained by plotting the distribution on semilog coordinates (Fig. 13). Here we see that we can cleanly fit a straight line to the tail of the distribution, implying an exponential

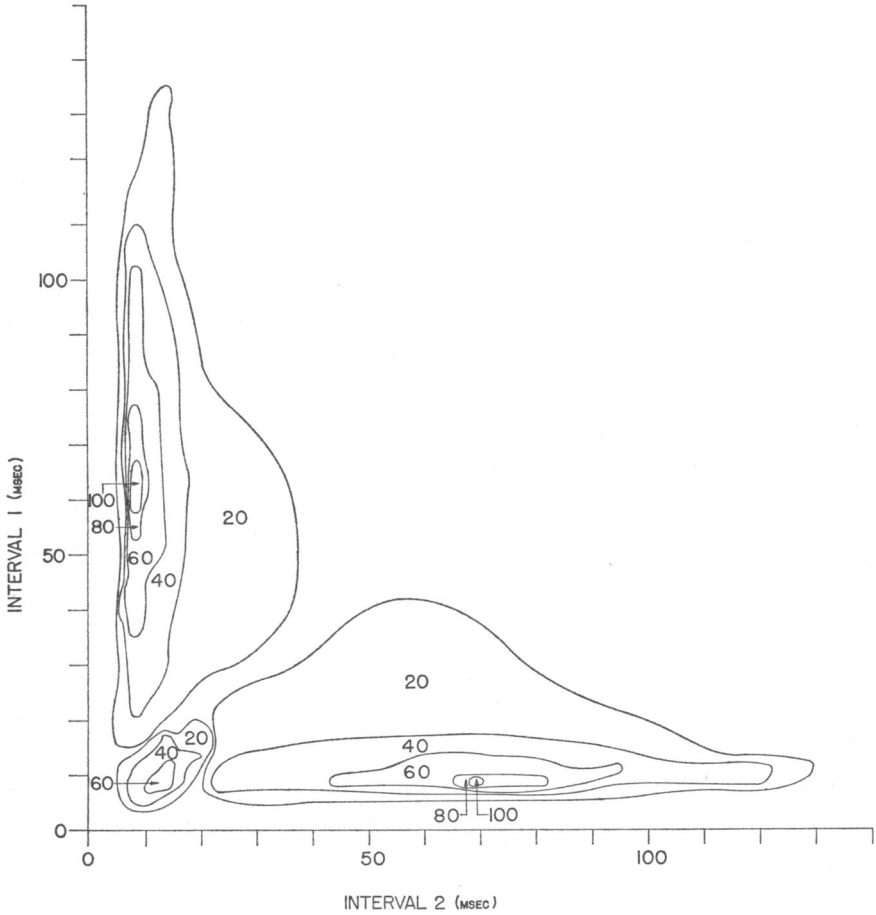

FIGURE 12 Joint interval histogram (contour plot). This contains all the information of the PIH, but also indicates the relation between an interval and the preceding one. The condition for independence between adjacent intervals is that the probability density profile along all horizontal and vertical lines has the same shape (differ from that along another line by only a constant ratio). Illumination approximately 0.6 mlm/cm², epoch 16 min well into steady-state response. *O. virilis*, unit 04145.

fall off. When we extrapolate past the moderate intervals, the histogram peaks above the exponential line. Reasoning from the pairwise dependency JIH plot we may hypothesize that moderate intervals have been preempted by the pairing process. At higher intensities, notch and peak phenomenon ("humping" on linear coordinates) all but disappears, overridden by the driving effect of high intensity stimulations (Fig. 13 B).

5. The standard deviation of the interval distribution is uniquely related to the mean (Fig. 11). This is seen to hold true for various values of illumination, and even

during the transient phase. It serves as the strongest evidence for the next point, which is necessarily somewhat subjective.

6. All distributions with the same mean, regardless of stimulus condition, have the same shape. Such a relationship indicates that all parameters in the stochastic model would be a constant times a single function of intensity and past history. Further, the mean is therefore a sufficient statistic. This follows because we are able

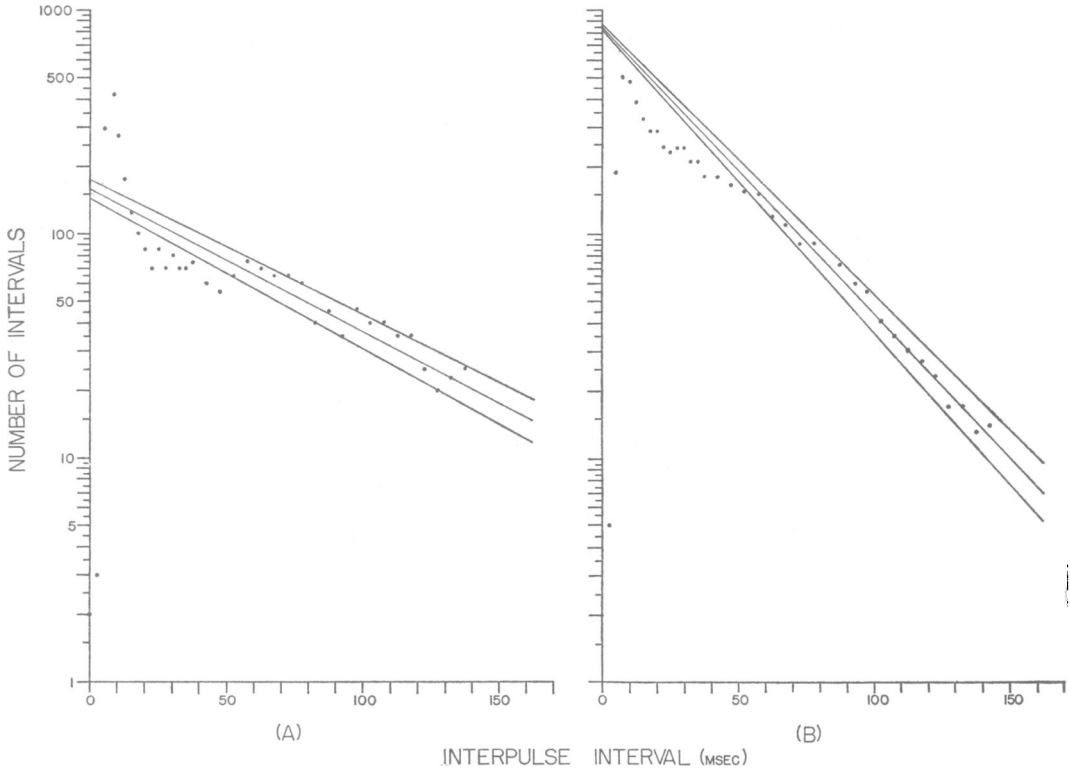

FIGURE 13 Semilogarithmic plots of pulse interval statistics in the steady state. A linear plot represents Poisson (random) statistics. Straight lines denote best fit (center line) and standard deviation bounds under Poisson assumption. Two different intensities represented, approximately (A) 0.6 mlm/cm² and (B) 3.0 mlm/cm². *O. virilis*, unit 04145.

to derive any statistic of the distribution if we know its mean. Therefore, the mean contains all of the message content, in an information theory sense, that the photoreceptor is communicating.

Under conditions of moderate to high intensity light driving, the photounit has a PIH whose exponential tail is consistent with the stochastic models advanced by a number of workers (13–21). The gamma distribution is used by some workers as a describing function (13, 11) and by others in a rational parameter model (18). The gamma distribution admits the linear relation between mean and standard deviation found in the photounit data (Fig. 11 B, where $M = 1$). On the other

hand, although the gamma preserves shape invariance under time scaling, this has not been corroborated by our data. Further, the gamma does not fit our type A distribution. If fitted to the tail, it does not produce sufficient numbers of pulses in the short interval.

The puzzling feature of pairing is not consistent with any model which has come to our attention. It is unquestionably important since it is often found in the dark resting state and is significantly present at moderate levels of illumination. It gives rise to the bimodal distributions seen in Fig. 2 a. Biederman-Thorson (11) has published data from crayfish neurons showing PIH with bimodal distributions. However, her data show little resemblance to ours. Gerstein (19) has published PIH's of spontaneous (resting?) activity in neurons of the vertebrate auditory cortex which show a striking resemblance to our data. Indeed, when driven by auditory clicks the change in shape of his unit is analogous to that found in the light-driven photounit.

CONCLUSION

This paper was based on averaging procedures; consequently, it ignored all fine structure of nerve pulse intervals. In characterizing many physical processes, averaging concepts have provided powerful models, e.g., statistical mechanics, thermodynamics, and so forth. Also in studying and designing communication systems, such conceptual tools as information and entropy have had brilliant success. Thus, workers in neurobiophysics have in their common intellectual heritage Bernoulli, Poisson, Willard Gibbs, and Shannon. It is not surprising that the obvious irregularities in nerve pulse interval data have been approached from the point of view of the orderly, powerful concepts of probability theory as applied to ergodic processes. Individual nerve cells have been noted to generate, as their unique hallmarks, sequences ranging from nearly periodic (20, 11) to the nearly random Poisson or Gaussian (13, 21). The outward appearances of most nerve pulse interval data invites comparison with stochastic processes.

Nonetheless, from the point of view of message content, statistical approaches alone, such as the present one, can do no more than establish an upper bound on possible channel capacity. Whether or not nerve cells are ambitious, efficient telegraphers is entirely unknown.

The problem is in part linguistic. In order to discuss variations, we need standards, and the most rigorous and compact current standards are provided by stochastic models. In this paper we have used the nerve pulse interval distribution as a descriptive language, believing such distributions important in characterizing the physical system as well as approaching the problem of message content.

Mr. Joshua Singer assisted in many of the experiments and supervised some of the data processing. In addition we are grateful for the help volunteered by patients of the McLean Hospital in carrying out numerical calculation and graphing.

This work was carried out under USPH Grant NB 04932.

Received for publication 23 November 1966.

REFERENCES

1. ROEDER, K. 1962. *Am. Zoologist.* **2**:105.
2. WELSH, J. H. 1934. *J. Cellular Comp. Physiol.* **4**:379.
3. HERMANN, H. T. 1964. *J. Exptl. Zool.* **155**:381.
4. HERMANN, H. T, and L. STARK. 1964. *J. Neurophysiol.* **26**:215.
5. PROSSER, C. L. 1934. *J. Cellular Comp. Physiol.* **4**:363.
6. KENNEDY, D. 1963. *J. Gen. Physiol.* **46**:551.
7. UTTAL, W., and H. KASPRZAK, *In* Proceedings 1962 Spring Joint Computer Conference, San Francisco. 159.
8. BRUNO, M. S., and D. KENNEDY. 1962. *Comp. Biochem. Physiol.* **6**:41.
9. HERMANN, H. T., and L. STARK. 1963. *Anat. Record.* **147**:209.
10. WIERSMA, C. A. G., and G. M. HUGHES. 1961. *J. Comp. Neurol.* **116**:209.
11. BIEDERMAN-THORSON, M. 1966. *J. Gen. Physiol.* **49**:597.
12. KENNEDY, D. 1958. *Am. J. Ophthalmol.* **46**:19.
13. KUFFLER, S. W., R. FITZHUGH, and H. B. BARLOW. 1957. **40**:683.
14. GROSSMAN, R. G., and L. J. VIERNSTEIN. 1961. *Science.* **134**:99.
15. GERSTEIN, G. L. 1962. *IRE (Inst. Radio Engrs.), Trans. Inform. Theory.* **8**:S137.
16. GERSTEIN, G. L., and B. MANDELBROT. 1964. *Biophys. J.* **4**:41.
17. WEISS, T. F. 1964. Massachusetts Institute of Technology Research Laboratory of Electronics Technical Report 418. *iii.*
18. STEIN, R. B. 1965. *Biophys. J.* **5**:173.
19. GERSTEIN, G. L. 1960. *Science.* **131**:1811.
20. FIRTH, D. R. 1966. *Biophys. J.* **6**:201.
21. RODIECK, R. W., N. Y.-S. KIANG, and G. L. GERSTEIN. 1962. *Biophys. J.* **2**:351.